Inorganic Chemistry

Communication

pubs.acs.org/IC

Role of the Alkali-Metal Cation Size in the Self-Assembly of Polyoxometalate-Monolayer Shells on Gold Nanoparticles

Yifeng Wang, Offer Zeiri, Shelly Sharet, and Ira A. Weinstock*

Department of Chemistry and the Ilse Katz Institute for Nanoscale Science & Technology, Ben Gurion University of the Negev, Beer Sheva 84105, Israel

Supporting Information

ABSTRACT: Polyoxometalate (POM)-monolayer stability constants, *K*, for three POM anions vary with the cation size, in the same order as that for increasing ion-pair formation with α-$SiW_{11}O_{39}^{8-}$ (**1**) in the early nucleation phase of monolayer self-assembly: $Li^+ < Na^+ < K^+ < Cs^+$. Cryo-TEM images demonstrating the use of the cation size to rationally control monolayer formation provide definitive evidence that the POM monolayers are electrostatically stabilized (ionic) shells, analogous in that respect to the monolayer walls of "hollow" POM-macroanion vesicles.

Cryogenic transmission electron microscopy (cryo-TEM) was recently used to directly image the intact "solution-state" structures of POM-protected silver (Ag)[1] and gold (Au)[2] nanoparticles (NPs) in water. Those findings represented a significant contribution to the establishment of structure/reactivity relationships for POM-protected metal(0) NPs,[3] a growing class of catalytically active nanostructures.

Data obtained using 14-nm-diameter Au NPs led to a structural model involving the extensive incorporation of countercations into the POM monolayer itself.[2] Accordingly, POM-protected metal NPs might be viewed as pivotal members in a continuum[4] of electrostatically stabilized structures ranging from two-dimensional arrays of POMs on planar surfaces[5] to the spherical single walls of hollow POM vesicles.[6] If this electrostatic model is correct, the stabilities of the POM monolayers on Au NPs should vary with the nature of the integrated countercation, just as do lattice enthalpies of crystalline POM salts and energies of cation association with POMs in solution.[7]

Now, using three representative POM anions and a series of alkali-metal cations, we show that POM-monolayer stability constants, *K*, vary with the size and properties of the cations in the same order as that observed for cation−anion association (ion-pair formation) in solution: $Li^+ < Na^+ < K^+ < Cs^+$.[8] Using α-$SiW_{11}O_{39}^{8-}$ (**1**; Figure 1A), it is then demonstrated that larger cations associate more extensively with the cluster anions even during the early "nucleation" stage of monolayer formation. On the basis of these findings, we then show how the alkali-metal cation size can now be used to rationally control the formation of ionic monolayer shells of cluster anions on Au NPs.

The above was achieved by the combined use of UV−vis spectroscopy and cryo-TEM imaging (Figure 1).[1,2,9] Panels C and D are cryo-TEM images of citrate- and **1**-protected Au NPs, respectively. While citrate ions are not observed, molecules of **1**, each containing 11 W atoms ($Z = 74$) for more effective imaging, are readily seen in panel D as a "ring" surrounding the perimeter of the Au core. Moreover, when **1** is added to solutions of the citrate-protected Au NPs, replacement of the organic ligands by metal oxide clusters causes a significant change in the surface plasmon resonance (SPR; panel B). This absorbance change can be used to quantify the thermodynamics and kinetics of POM-monolayer assembly.

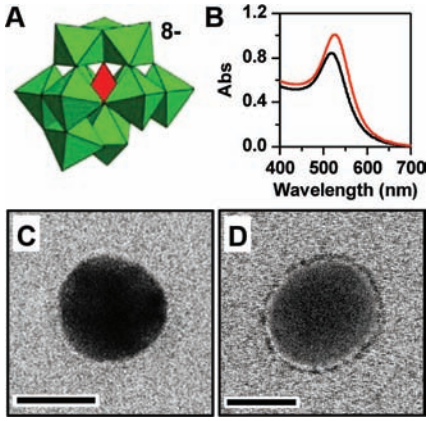

Figure 1. Reaction of **1** with a citrate-stabilized, 14-nm-diameter Au NP: (A) structure of **1** (polyhedral notation); (B) UV−vis spectra of citrate-stabilized Au NPs before (black) and after (red) monolayer formation by **1**; (C and D) cryo-TEM images of citrate- and **1**-protected Au NPs, respectively. Bar = 10 nm.

In Figure 2, absorbance values (526 nm) are plotted as a function of the M_8**1** concentration, where M = Li^+, Na^+, K^+, and Cs^+. For each plot, Au NPs were prepared using citrate salts containing the same cation as that in the POM salt, so that each reaction mixture contained only a *single type of cation*. As the M_8**1** concentrations increase, absorbance increases until reaching a plateau (a Langmuir type I isotherm). Fitting of the data to a function describing the dependence of absorbance on [M_8**1**] (red curves; see the Supporting Information, SI) gives the monolayer stability constants, *K*, in Table 1. Analogous constants were obtained for $M_9[AlW_{11}O_{39}]$ (M_9**2**; the α isomer for M = K^+ and α−β mixtures for the other

Received: February 26, 2012
Published: April 19, 2012

   dx.doi.org/10.1021/ic300431a | *Inorg. Chem.* 2012, 51, 7436−7438

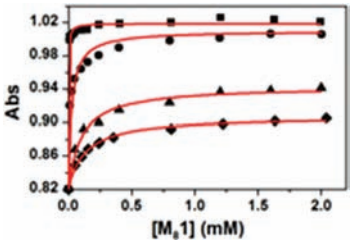

Figure 2. Adsorption isotherms at ca. pH 6.3 for reactions of citrate-protected Au NPs ($3.1 \pm 0.7 \times 10^{-9}$ M) with M_8**1**, where M = alkali-metal cation. These are (from bottom to top) Li^+ (♦), Na^+ (▲), K^+ (●), and Cs^+ (■). The red curves are fits to eq S4 in the SI.

Table 1. Stability Constants for POM Monolayers[a]

	Langmuir stability constants, K (mM^{-1})[a]				
POM	Li^+	Na^+	K^+	TMA^+ [b]	Cs^+
1	7.4 ± 1.6	10.3 ± 0.6	79 ± 13	138 ± 5	750 ± 260
2	9.5 ± 0.5	14.9 ± 0.7	150 ± 13	200 ± 40	*c*
3	<0.4	0.7 ± 0.1	5.2 ± 1.3	2430 ± 790	2530 ± 180

[a]Uncertainties are estimated by curve fitting; see the SI. [b]For clarification, the isotherm for TMA^+ is provided separately, as Figure S2 in the SI. [c]Cs_9**2** is poorly soluble.

cations) and for salts of the Preyssler ion $M_{14}[NaP_5W_{30}O_{110}]$ (M_{14}**3**). For all three anions, the stability constants, K, increase in the order $Li^+ < Na^+ < K^+ < TMA^+ < Cs^+$ (Table 1).[10]

This trend parallels the general tendency of POMs (and other anions)[7,8,11] to associate (i.e., form ion pairs) more strongly with larger alkali-metal cations, which, in water, possess *smaller* hydrated radii and smaller energies of hydration (Table 2, columns 1–4). (While TMA^+ is structurally unique relative to the other cations, it fits within the overall trends in Table 1.) Similarly, monolayer stability constants, K, increase with alkali-metal cation size (crystallographic radii) because of the more favorable electrostatic interactions that result from shorter distances between the POM anions and the smaller *hydrated* countercations and/or from the smaller energetic costs associated with the cations' partial dehydration. These issues also play a role in the well-known decrease in the aqueous POM-salt solubility as alkali-metal countercations are varied from Li^+ to Cs^+.

Table 2. Cation Properties and Ion Pairing during Nucleation of 1 on the Au Surface

cation	ionic radius,[a] Å	hydrated radius,[a] Å	hydration energy,[a] kcal mol^{-1}	k_i [b] M^{-1} s^{-1}	effective POM charge[c]
Li^+	0.60	3.40	−123	0.5 ± 0.1	−8
Na^+	0.95	2.76	−97	0.7 ± 0.1	−7.9
K^+	1.33	2.32	−77	4.4 ± 0.4	−7.5
TMA^+	3.22	~6.3	−52	21 ± 1	−7.1
Cs^+	1.69	2.28	−63	105 ± 6	−6.7

[a]Values for Li^+, Na^+, K^+, and Cs^+ are from ref 11 and those of TMA^+ are from refs 12 and 13. [b]Error is based on ≥3 identical experiments; see the caption to Figure 3. [c]The effective charge of **1** in the presence of Li^+ (5.4 mM) was set at 8− (no ion pairing) to obtain *relative* values for the larger cations.

When **1** and $AlW_{11}O_{39}^{9-}$ (**2**) are compared, the K values are consistently larger for the more negatively charged anion. As previously reported,[2] the K values for a series of plenary and monodefect Keggin anions increased monotonically with the anion charge (from 5− to 9−), suggesting that the defect site provides no unique stability to the POM monolayer. The importance of the POM charge is further supported using the Brønsted acid–base properties of **1**. Adjusting the pH from 6.3 to 4.6 converts **1** (Na^+ electrolyte) to its monoprotonated form, $[\alpha\text{-}HSiW_{11}O_{39}]^{7-}$ (pK_a = 5.2,[14] with protonation occurring at the formally $W-O^-$ ligands at the defect site). The resultant K value (ca. 7 mM^{-1}) is close to the value of 8 mM^{-1} for unprotonated $[\alpha\text{-}PW_{11}O_{39}]^{7-}$ (see Figure S3 in the SI).

The more favorable association of POMs with larger cations implied by the data in Table 1 was confirmed by evaluating the relative extents of ion pairing with **1** in the early nucleation[9a] stage of monolayer formation. For this, the NPs *themselves* were used as SPR "sensors" to detect the initial rates of citrate place exchange[15] by **1** at the Au surface. The relative extents of ion pairing follow directly from the exponential dependence of the rate on the *net charge* of the approaching anions: The ζ potential of the citrate-protected Au particles is −39 ± 4 mV, indicative of a negative potential at the slipping plane (ca. 5 nm from the Au surface; see Table S1 in the SI). This potential increases to a value of $\Psi = \zeta/0.37$ at the Stern layer (ca. 0.5 nm from the Au surface),[16] presenting an energetic barrier shown to be approximated[17] by $-q\Psi/RT$, where q is the net charge of the approaching anion (eq 1).

$$k_i = k_0 \exp(-q\Psi/RT) \quad (1)$$

In eq 1, k_i is the rate constant for POM adsorption at the Au surface (nucleation) and k_0 is the rate constant in the absence of a potential-energy barrier. Hence, an increase in cation association with **1** *within the double layer* should increase the rates of POM nucleation at the Au surface (Figure 3).

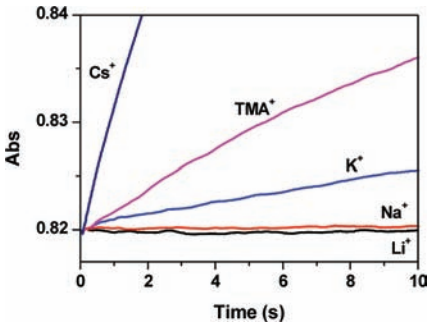

Figure 3. SPR responses (at 526 nm) during the initial nucleation phase of monolayer formation by M_8**1**. Data were acquired after rapid (stopped-flow) mixing of lithium citrate-stabilized 14-nm-diameter Au NPs ($6.2 \pm 1.3 \times 10^{-9}$ M, and 6.0 mM Li^+) with equal volumes of 0.6 mM M_8**1**, where M = Li^+ Na^+, K^+, TMA^+, and Cs^+ (4.8 mM in each). Each curve is an average of 20 traces, and the initial rates were determined from the early linear portions of each curve, ca. 1 s for K^+ and TMA^+ and 0.2 s for Cs^+.

Rate constants k_i were obtained from the early portions of the curves in Figure 3. The k_i values (column 5 of Table 2) increase markedly with the cation size. Relative net charges, calculated using eq 1 (column 6; see the SI), decrease from Li^+ to Cs^+, reflecting greater degrees of cation association with **1** in the diffuse region (<5 nm) from the Au surface. Hence, even at the earliest stage of monolayer assembly, the larger cations (including TMA^+) associate more extensively with **1**. This provides an independent line of evidence that the stability

dx.doi.org/10.1021/ic300431a | *Inorg. Chem.* 2012, 51, 7436–7438

constants, K, in Table 1 similarly reflect more favorable interactions of POM anions with the larger cations.

Definitive support for the stabilizing role of cation−anion interactions in POM-monolayer shells was provided by cryo-TEM. The K value for the Li^+ salt of the Preyssler ion (**3** in Table 1) is ca. 0.4 mM^{-1}. As such, very little POM-monolayer formation (i.e., ca. 2%) should occur when a lithium citrate-protected Au NP solution is made 0.05 mM in Li_{14}**3**. As expected, no POMs are observed at the perimeter of the Au core (Figure 4A). By contrast, on the basis of the large K value

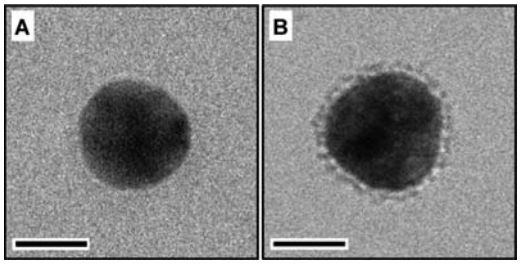

Figure 4. Cryo-TEM images of citrate-protected Au NPs after reaction with Li^+ and Cs^+ salts of **3**: (A) Li_{14}**3** (0.05 mM) in lithium citrate-protected Au NPs; (B) Cs_{14}**3** (0.05 mM) in cesium citrate-protected Au NPs. Bar = 10 nm.

of 2530 mM^{-1} for the Cs^+ salt of **3**, the same concentration of Cs_{14}**3** (0.05 mM in a cesium citrate-protected Au NP solution) should result in complete (99%) monolayer formation. The predicted structure is confirmed by cryo-TEM (Figure 4B).

In summary, the role of cations in the formation and stability of POM monolayers on 14-nm-diameter Au NPs has been evaluated using three POM anions and a series of alkali-metal cations and TMA^+. Two primary lines of evidence demonstrate that the monolayer stability is a function of cation−anion interactions in the POM-protecting shell: (1) monolayer stability constants, K, increase as the hydrated radii and hydration energies of the alkali-metal cations *decrease* from Li^+ to Cs^+, and (2) larger alkali-metal cations (with smaller hydrated radii) associate more extensively (i.e., more energetically favorably) with **1** even in the early nucleation phase of monolayer formation. These findings provide definitive support for a structural model involving an electrostatically stabilized (ionic) shell involving POM anions and structurally integrated cations.[18]

Finally, cryo-TEM images directly confirm that the quantitative information provided here can be used to predict and rationally control the self-assembly of metal oxide cluster-anion-protecting ligand shells on Au NPs.

■ ASSOCIATED CONTENT

Supporting Information

Experimental details, cryo-TEM images, thermodynamic data, and additional discussion. This material is available free of charge via the Internet at http://pubs.acs.org.

■ AUTHOR INFORMATION

Corresponding Author

*E-mail: iraw@bgu.ac.il.

Notes

The authors declare no competing financial interest.

■ ACKNOWLEDGMENTS

I.A.W. thanks the ISF (Grants 248/09 and 1667/09) and I-CORE/ISF (Grant 152/11) for support, Maya Bar-Sadan for assistance with image processing, and Sivil Kopilevich for the cover graphic.

■ REFERENCES

(1) Neyman, A.; Meshi, L.; Zeiri, L.; Weinstock, I. A. *J. Am. Chem. Soc.* **2008**, *130*, 16480−16481.

(2) Wang, Y.; Neyman, A.; Arkhangelsky, E.; Gitis, V.; Meshi, L.; Weinstock, I. A. *J. Am. Chem. Soc.* **2009**, *131*, 17412−17422.

(3) (a) Hsu-Yao, T.; Browne, K. P.; Honesty, N.; Tong, Y. J. *Phys. Chem. Chem. Phys.* **2011**, *13*, 7433−7438. (b) Li, S.; Yu, X.; Zhang, G.; Ma, Y.; Yao, J.; Keita, B.; Louis, N.; Zhao, H. *J. Mater. Chem.* **2011**, *21*, 2282−2287. (c) Graham, C. R.; Ott, L. S.; Finke, R. G. *Langmuir* **2009**, *25*, 1327−1336. (d) Troupis, A.; Triantis, T.; Hiskia, A.; Papaconstantinou, E. *Eur. J. Inorg. Chem.* **2008**, 5579−5586. (e) Chojak, M.; Kolary-Zurowska, A.; Renata, W.; Miecznikowski, K.; Karnicka, K.; Palys, B.; Marassi, R.; Kulesza, P. J. *Electrochim. Acta* **2007**, *52*, 5574−5581. (f) Maayan, G.; Neumann, R. *Chem. Commun.* **2005**, 4595−4597. (g) Mandal, S.; Selvakannan, P. R.; Pasricha, R.; Sastry, M. *J. Am. Chem. Soc.* **2003**, *125*, 8440−8441. (h) Troupis, A.; Hiskia, A.; Papaconstantinou, E. *Angew. Chem., Int. Ed.* **2002**, *41*, 1911−1914. (I) Lin, Y.; Finke, R. G. *J. Am. Chem. Soc.* **1994**, *116*, 8335−8353.

(4) Wang, Y.; Weinstock, I. A. *Dalton Trans.* **2010**, *39*, 6143−6152.

(5) (a) Ge, M.; Zhong, B.; Klemperer, W. G.; Gewirth, A. A. *J. Am. Chem. Soc.* **1996**, *118*, 5812−5813. (b) Aparicio-Angles, X.; Clotet, A.; Bo, C.; Poblet, J. M. *Phys. Chem. Chem. Phys.* **2011**, *13*, 15143−15147. (c) Keita, B.; Nadjo, L. *J. Electroanal. Chem.* **1987**, *227*, 265−270.

(6) (a) Liu, T.; Langston, M. L. K.; Li, D.; Pigga, J. M.; Pichon, C.; Todea, A. M.; Müller, A. *Science* **2011**, *331*, 1590−1592. (b) Liu, T. *Langmuir* **2010**, *26*, 9202−9213.

(7) (a) Antonio, M. R.; Nyman, M.; Anderson, T. M. *Angew. Chem., Int. Ed.* **2009**, *48*, 6136−6140. (b) Pigga, J. M.; Kistler, M. L.; Shew, C.-Y.; Antonio, M. R.; Liu, T. *Angew. Chem., Int. Ed.* **2009**, *48*, 6538−6542. (c) Leroy, F.; Miro, P.; Poblet, J. M.; Bo, C.; Avalos, J. B. *J. Phys. Chem. B* **2008**, *112*, 8591−8599.

(8) (a) Marcus, Y.; Hefter, G. *Chem. Rev.* **2006**, *106*, 4585−4621. (b) Swaddle, T. W. *Chem. Rev.* **2005**, *105*, 2573−2608. (c) Grigoriev, V. A.; Cheng, D.; Hill, C. L.; Weinstock, I. A. *J. Am. Chem. Soc.* **2001**, *123*, 5292−5307.

(9) (a) Wang, Y.; Zeiri, O.; Neyman, A.; Stellacci, F.; Weinstock, I. A. *ACS Nano* **2012**, *6*, 629−640. (b) Wang, Y.; Zeiri, O.; Gitis, V.; Neyman, A.; Weinstock, I. A. *Inorg. Chim. Acta* **2010**, *363*, 4416−4420.

(10) This trend cannot be attributed to alkali-metal cation pairing with citrate. See the data and discussion in the SI.

(11) Weinstock, I. A. *Chem. Rev.* **1998**, *98*, 113−170.

(12) García-Tarrés, L.; Guàrdia, E. *J. Phys. Chem. B* **1998**, *102*, 7448−7454.

(13) Aue, D. H.; Webb, H. M.; Bowers, M. T. *J. Am. Chem. Soc.* **1976**, *98*, 318−329.

(14) Guo, S.-X.; Mariotti, A. W. A.; Schlipf, C.; Bond, A. M.; Wedd, A. G. *Inorg. Chem.* **2006**, *45*, 8563−8574.

(15) Nucleation on the Au surface is first-order in [POM], while citrate is labile, and its Langmuir constant is ca. 1/10000 that of **1**.

(16) Riley, J. Charge in Colloidal Systems. In *Colloid Science: Principles, Methods and Applications*; Cosgrove, T., Ed.; Blackwell Publishing, Ltd.: Oxford, U.K., 2005; pp 14−35.

(17) (a) MacRitchie, F. Physical Processes at Interfaces. In *Chemistry at Interfaces*; Academic Press, Inc.: San Diego, 1990; pp 156−165. (b) MacRitchie, F.; Alexander, A. E. *J. Colloid Sci.* **1963**, *18*, 464−469. (c) Hartley, G. S.; Roe, J. W. *Trans. Faraday Soc.* **1940**, *35*, 101−109.

(18) POM−Au interactions are also important. See: Sharet, S.; Sandars, E.; Wang, Y.; Zeiri, O.; Neyman, A.; Meshi, L.; Weinstock, I. A. *Dalton Trans.*, DOI: 10.1039/C2DT30592E.